

Coupled-rearrangement-channel Gaussian-basis variational method for trinucleon bound states

H. Kameyama and M. Kamimura

Department of Physics, Kyushu University, Fukuoka 812, Japan

Y. Fukushima

Department of Applied Physics, Fukuoka University, Fukuoka 814, Japan

(Received 1 February 1989)

To the ${}^3\text{H}$ and ${}^3\text{He}$ ground states, we apply the coupled-rearrangement-channel variational method with Gaussian-basis functions which has successfully been used in precise calculations of muonic molecular ions, Coulomb-interacting three-body systems. The trinucleon wave function is decomposed into angular-momentum-projected three-body channels as done in the Faddeev equations method, but the interaction is fully incorporated with no partial-wave decomposition. The radial part of the channel amplitudes is expanded with a sufficient number of Gaussian-tail basis functions of the Jacobi coordinates. The Gaussian ranges are taken to be geometrical progressions which run from very short ranges through large enough ones. This *ab initio* variational approach is found to describe accurately both the short-range correlations and the asymptotic behavior. The Argonne V_{14} potential is used as an example of realistic two-nucleon interactions; for ${}^3\text{He}$, the Coulomb potential is included nonperturbatively. The calculation reproduces precisely the results of the Faddeev calculations for ${}^3\text{H}$ and ${}^3\text{He}$ for binding energy, probabilities of the S , S' , P , and D states, and the S - and D -wave asymptotic normalization constants. Convergence of the present results is seen at a much smaller number of the three-body channels than in the Faddeev calculations. This is because the interaction is truncated in the angular momentum space in the Faddeev calculations but the full interaction is taken in the present method.

I. INTRODUCTION

It is well known that realistic two-nucleon potentials which fit the nucleon-nucleon data underbind the triton by about 1 MeV compared with the experimental value of 8.48 MeV. Recent Faddeev calculations, however, show that further inclusion of a three-nucleon potential with an appropriate strength can explain the energy.¹⁻⁴ Convergence of the calculated triton binding energy with increasing number of the three-body channels, however, does not seem satisfactory when the three-body potential is incorporated.^{2,4} For example, the energy calculated by Ishikawa and Sasakawa⁴ is 7.70, 8.61, 8.33, and 8.42 MeV with 5, 18, 26, and 34 channels, respectively, when the Tucson-Melborne three-body potential for two-pion exchange⁵ ($\Lambda=700$ MeV) is employed together with the Argonne V_{14} potential (AV14).⁶ It is likely that such a slow convergence is due to the truncation of the partial waves of the two- (three-)nucleon potentials; the partial waves, say j , of the interactions are restricted to $j \leq 1^+$ (${}^1S_0, {}^3S_1$ - 3D_1), $j \leq 2$, $j \leq 3$, and $j \leq 4$ in the calculations with 5, 18, 26, and 34 channels, respectively.

On the other hand, variational methods do not necessarily require such a truncation of the partial waves of the interactions. Results of variational calculations,⁷⁻¹² however, are not as precise as those of the recent Faddeev calculations, especially in regard to the asymptotic behavior of the three-body wave function.¹³ Generally speaking, it is a difficult task to provide a set of variational basis functions which are tractable in numerical calculations and suitable both for the short-range repulsion re-

gion and for the asymptotic tail region.

The purpose of this paper is to solve this difficulty in the variational approach to the trinucleon bound states and to perform an accurate calculation which utilizes the full interaction with no partial-wave expansion. With this aim, we employ the coupled-rearrangement-channel Gaussian-basis variational method which has been developed by one of the authors (MK) (Ref. 14) in the study of muonic molecular ions, Coulomb-interacting three-body systems in which mass is not very different among the three particles. A successful example is seen in a precise calculation of the molecular ion $dt\mu^-$ (deuteron + triton + muon); an accuracy of seven digits in the energy value was achieved with a short computation time for all five bound states including the very weakly bound one which is a key to the muon catalyzed fusion.¹⁵

In Ref. 14, the $dt\mu^-$ wave function was expanded with Jacobi-coordinate three-body basis functions which spanned the three rearrangement channels ($t\mu$ - d , $d\mu$ - t , and dt - μ). Radial functions of each coordinate are expressed in terms of Gaussian-tail functions whose ranges are over a very small value through a large enough one. A typical three-body basis function on a rearrangement channel whose Jacobi coordinates are \mathbf{x} and \mathbf{y} looks like

$$x^l \exp[-(x/x_n)^2] y^L \exp[-(y/y_N)^2] [Y_l(\hat{x}) \otimes Y_L(\hat{y})]_{JM}, \quad (1.1)$$

where l (L) is the angular momentum associated with the coordinate \mathbf{x} (\mathbf{y}). Expansion coefficients of the basis functions were determined by the Rayleigh-Ritz varia-

tional principle through the diagonalization of the Hamiltonian with Coulomb potentials among d , t , and μ^- . Use of the above basis functions makes it very easy to transform them onto other rearrangement channels, and therefore energy matrix elements can be calculated fully analytically. With the angular momenta $l, L \leq 4$ and an appropriate set of the ranges (x_n) and (y_N) which were chosen to be geometrical progressions, the basis functions were found to be suited for a precise description of the five bound states ($J=0, 1$, and 2) both in the asymptotic region and in the short-range region where the amplitude of the d - t relative motion is heavily suppressed by the repulsive Coulomb potential; the number of the basis functions is about 1400–1800 to have a seven-digit accuracy in energy.

For the three-nucleon systems, the Gaussian ranges and the angular momenta of the three-body basis functions should be chosen so as to be suitable for the short-range repulsion and the strong tensor force, as well as to be appropriate for the asymptotic behavior. Before entering the three-body calculation, we first tested the usefulness of our Gaussian-basis functions for the deuteron ground state with the Reid soft-core potential.¹⁶ The S - and D -wave radial components, $u(r)$ and $w(r)$, respectively, were described with 20 Gaussian-tail functions:

$$\begin{aligned} \frac{u(r)}{r} &= \sum_{n=1}^{20} a_n \exp[-(r/r_n)^2], \\ \frac{w(r)}{r} &= \sum_{n=1}^{20} b_n r^2 \exp[-(r/r_n)^2]. \end{aligned} \quad (1.2)$$

Here the series $\{r_n; n=1 \sim 20\}$ are chosen to be *geometrical* progressions with $r_1=0.05$ fm and $r_{20}=20.0$ fm for $u(r)$, and $r_1=0.1$ fm and $r_{20}=18.0$ fm for $w(r)$; the density of the basis functions is very high in the short-range region where the wave function changes rapidly. The coefficients (a_n) and (b_n) are determined by the Rayleigh-Ritz variational principle. The sum in Eq. (1.2) appears to be coherent for long-range Gaussians, but heavily destructive for short-range ones with $r_n \lesssim 1$ fm. The calculated result completely reproduced all the values of the deuteron quantities which are tabulated in Ref. 16, including the five-figure numbers of $u(r)$ and $w(r)$ and their derivatives given for $r < 13$ fm. Also, as seen in Fig. 1, the asymptotic behavior of $u(r)$ and $w(r)$ is accurately described up to a sufficiently large distance; the relative error is $\sim 0.1\%$ at $r \sim 30$ fm and $\sim 1\%$ at $r \sim 43$ fm. This high accuracy may be more than one expects from ‘‘Gaussian-tail’’ basis functions, especially in the asymptotic region. Therefore, it may not be unreasonable to consider that the coupled-rearrangement-channel variational method in which each basis function takes the form of (1.1) will also work for the trinucleon systems as far as a good choice is made for the Gaussian ranges.

The three-nucleon wave function of our method is described with a symmetric sum of the three rearrangement-channel amplitudes which are angular-momentum projected with respect to each Jacobian coordinate [cf. (1.1)]. Thus, our wave function is rather simi-

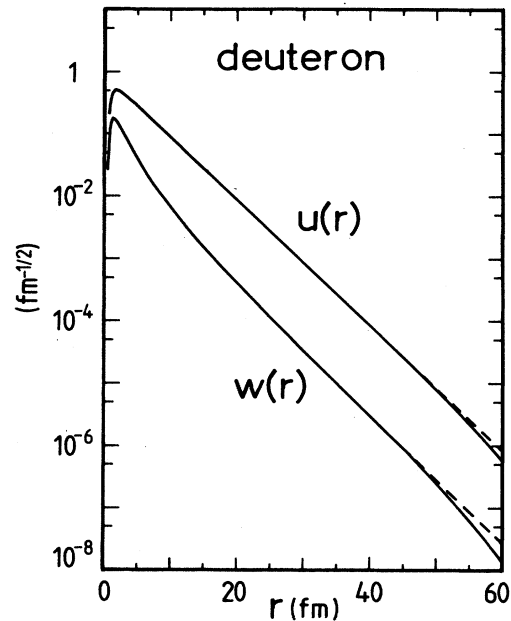


FIG. 1. Variationally calculated deuteron wave function with the use of the Gaussian-tail basis functions of Eqs. (1.2). The Reid soft-core potential (Ref. 16) is used. The solid curves show our results and the dashed curves are the exact solution given in Ref. 16.

lar in form to the Faddeev wave function; also, calculations are classified according to the number of three-body angular-momentum channels employed. We can therefore examine convergence of calculated results with respect to increasing number of channels in the same manner as the Faddeev calculations. However, it is to be noted that, in our method, the partial-wave expansion of the nucleon-nucleon interaction is not necessary, and any truncation of the partial waves is not taken at all; this is one of the major differences between this method and the Faddeev one. It will later be shown that the use of the full interaction in our framework gives rise to a convergence of the calculated results at a much smaller number of channels than in the Faddeev calculations; in this paper, this is studied without three-body potentials.

The variational basis functions in the form of (1.1) for three-particle systems was successfully applied some ten years ago by two of the authors (Y.F. and M.K.) (Ref. 17) to the three-alpha-cluster resonating-group calculation of the ^{12}C nucleus in which each alpha cluster is assumed to have the $(0s)^4$ configuration and the 12 nucleons are antisymmetrized; but use was made of effective nucleon-nucleon interactions instead of realistic ones. Then, Matsuse and Hoshi¹⁸ utilized a similar type of basis function for the triton ground state with the Reid soft-core potential (RSC5 with 1S_0 and S_1 - 3D_1) and obtained a binding energy of 6.1 MeV, which is smaller by 1 MeV than the result of the Faddeev five-channel calculation; the number of basis functions was too small. It may be said that our variational approach has extensively been

refined in the study of muonic molecular ions¹⁴ as mentioned above.

Construction of the paper is as follows. In Sec. II, the framework of our method is presented. The model space of the calculation is introduced in Sec. III. Some formulae for the trinucleon asymptotic behavior are summarized in Sec. IV. Calculated results for ³H are given in Sec. V. We discuss the binding energy, the probabilities of the *S*, *S'*, *P*, and *D* states, and the asymptotic normalization constants. Convergence of these quantities with increasing number of channels is examined. The results are compared with those of the Faddeev calculations. The same is done for ³He in Sec. VI. A summary and concluding remarks are given in Sec. VII.

II. NUMERICAL METHODS

We use the Jacobi coordinates (Fig. 2):

$$\mathbf{x}_i = \mathbf{r}_j - \mathbf{r}_k, \quad (2.1)$$

$$\mathbf{y}_i = \mathbf{r}_i - \frac{1}{2}(\mathbf{r}_j + \mathbf{r}_k), \quad (2.2)$$

where *i*, *j*, and *k* denote cyclic permutation. In this paper we do not consider three-body potentials. The total Hamiltonian for the system is then of the form

$$H = T + V(\mathbf{x}_1) + V(\mathbf{x}_2) + V(\mathbf{x}_3), \quad (2.3)$$

where *T* is the kinetic energy operator and *V*(**x**) is the

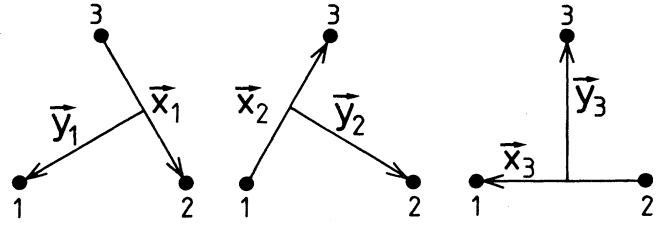


FIG. 2. Three rearrangement channels of the trinucleon system and their Jacobi coordinates.

two-body interaction including the Coulomb force. The full interaction is taken with no partial-wave decomposition. The isospin mixing between $T = \frac{1}{2}$ and $\frac{3}{2}$ due to the Coulomb force in the ³He nucleus is ignored in this work. The total wave function for the trinucleon bound state with $J = T = \frac{1}{2}$, say Ψ , is described as a symmetric sum of the three rearrangement-channel amplitudes as functions of the Jacobian coordinates of the channels:

$$\Psi = \Phi(\mathbf{x}_1, \mathbf{y}_1) + \Phi(\mathbf{x}_2, \mathbf{y}_2) + \Phi(\mathbf{x}_3, \mathbf{y}_3). \quad (2.4)$$

We expand the amplitudes $\Phi(\mathbf{x}_i, \mathbf{y}_i)$ in terms of the three-body angular-momentum channels which are specified by α :

$$\Phi(\mathbf{x}_i, \mathbf{y}_i) = \sum_{\alpha} \psi_{\alpha}(x_i, y_i) \mathcal{Y}_{\alpha}(jk, i), \quad (2.5)$$

$$\mathcal{Y}_{\alpha}(jk, i) = [[Y_{l_{\alpha}}(\hat{x}_i) \otimes Y_{L_{\alpha}}(\hat{y}_i)]_{\Lambda_{\alpha}} \otimes [\chi_{s_{\alpha}}(jk) \otimes \chi_{1/2}(i)]_{\Sigma_{\alpha}}]_{JM} [\eta_{t_{\alpha}}(jk) \otimes \eta_{1/2}(i)]_{TT_2}, \quad (2.6)$$

where l_{α} is the orbital angular momentum of particles *j* and *k*, L_{α} is the orbital angular momentum of particle *i* relative to the center of mass of particles *j* and *k*, Λ_{α} is the total orbital angular momentum of the three-particle system, s_{α} is the spin angular momentum of particles *j* and *k*, Σ_{α} is the total spin of the three-particle system, and t_{α} is the isospin of particles *j* and *k*. The Pauli principle between particles *j* and *k* requires $l_{\alpha} + s_{\alpha} + t_{\alpha} = \text{odd}$. In Eq. (2.6), the *Y*'s are the spherical harmonics, and the χ 's and η 's are, respectively, the spin and isospin functions. We take the *L-S* coupling representation for the sake of simplicity in the space-coordinate transformation; the *j-J* coupling scheme is not necessary since the partial-wave expansion of interactions is not taken in this method.

Unknown radial amplitudes $\psi_{\alpha}(x_i, y_i)$ are expanded in terms of basis functions associated with the radial coordinates x_i and y_i :

$$\psi_{\alpha}(x_i, y_i) = \sum_{n_{\alpha}=1}^{n_{\alpha}^{\max}} \sum_{N_{\alpha}=1}^{N_{\alpha}^{\max}} A_{\alpha n_{\alpha} N_{\alpha}} \phi_{n_{\alpha} l_{\alpha}}(x_i) u_{N_{\alpha} L_{\alpha}}(y_i). \quad (2.7)$$

The total wave function Ψ is then expressed in the form

$$\Psi = \sum_{\bar{\alpha}} A_{\bar{\alpha}} [\Phi_{\bar{\alpha}}(\mathbf{x}_1, \mathbf{y}_1) + \Phi_{\bar{\alpha}}(\mathbf{x}_2, \mathbf{y}_2) + \Phi_{\bar{\alpha}}(\mathbf{x}_3, \mathbf{y}_3)], \quad (2.8)$$

where $\bar{\alpha} \equiv \{\alpha, n_{\alpha}, N_{\alpha}\}$ and

$$\Phi_{\bar{\alpha}}(\mathbf{x}_i, \mathbf{y}_i) = \phi_{n_{\alpha} l_{\alpha}}(x_i) u_{N_{\alpha} L_{\alpha}}(y_i) \mathcal{Y}_{\alpha}(jk, i). \quad (2.9)$$

The coefficients $A_{\bar{\alpha}}$ and the eigenenergy *E* are determined by the following equations derived from the Rayleigh-Ritz variational principle:

$$\langle \Phi_{\bar{\alpha}}(\mathbf{x}_2, \mathbf{y}_1) | H - E | \Psi \rangle = 0 \quad (2.10)$$

for all $\bar{\alpha}'$. They lead to a generalized eigenvalue problem:

$$\sum_{\bar{\alpha}} (H_{\bar{\alpha}'\bar{\alpha}} - EN_{\bar{\alpha}'\bar{\alpha}}) A_{\bar{\alpha}} = 0, \quad (2.11)$$

with

$$\begin{pmatrix} H_{\bar{\alpha}'\bar{\alpha}} \\ N_{\bar{\alpha}'\bar{\alpha}} \end{pmatrix} = \langle \Phi_{\bar{\alpha}'}(\mathbf{x}_1, \mathbf{y}_1) | (H_1^H) | \Phi_{\bar{\alpha}}(\mathbf{x}_1, \mathbf{y}_1) + \Phi_{\bar{\alpha}}(\mathbf{x}_2, \mathbf{y}_2) + \Phi_{\bar{\alpha}}(\mathbf{x}_3, \mathbf{y}_3) \rangle, \quad (2.12)$$

where $H_{\bar{\alpha}\bar{\alpha}'} = H_{\bar{\alpha}'\bar{\alpha}}$ and $N_{\bar{\alpha}\bar{\alpha}'} = N_{\bar{\alpha}'\bar{\alpha}}$. The symmetrized basis functions in Eq. (2.8) are not orthogonal to one another unless the quantum numbers $(\Lambda_{\alpha}, \Sigma_{\alpha})$ are different between them.

A crucial problem of the variational method is how to choose the radial functions $\phi_{n_{\alpha}l_{\alpha}}(x)$ and $u_{N_{\alpha}L_{\alpha}}(y)$. A typical example of them would be the eigenfunctions of a harmonic oscillator potential, but they are not suited for a precise description of the short-range correlation and the asymptotic behavior. As done successfully in Ref. 14, we employ the Gaussian-tail functions whose ranges are of geometrical progression (subscript α is omitted):

$$\begin{aligned} \phi_{n_l}(x) &= x^l \exp[-(x/x_n)^2], \\ x_n &= x_{\min} a^{n-1} \quad (n=1-n_{\max}) \\ u_{NL}(y) &= y^L \exp[-(y/y_N)^2], \\ y_N &= y_{\min} b^{N-1} \quad (N=1-N_{\max}). \end{aligned} \quad (2.13)$$

The geometrical progressions are useful in optimizing the ranges with a small number of free parameters. Nonlinear variational parameters $(n_{\max}, x_{\min}, x_{\max})$ and $(N_{\max}, y_{\min}, y_{\max})$ may be chosen differently for individual channels α (cf. Sec. III); here, $x_{\max} = x_{n_{\max}}$ and $y_{\max} = y_{N_{\max}}$. For many sets of the nonlinear parameters we solve $A_{\bar{\alpha}}$'s and E through Eqs. (2.11) and try to find as large a binding energy as possible by optimizing the parameters.

Distribution of the Gaussian ranges of geometrical progression is dense at small ranges, which is suited for making the wave function correlate with soft-core potentials. The "fast" damping of the Gaussian tails is not a problem since we can make x_{\max} and y_{\max} much longer than the size of ${}^3\text{H}$ (${}^3\text{He}$) and expect the long-range basis functions to work coherently; note the excellent example for the deuteron wave function in Fig. 1.

With the use of the Gaussian tails, rather than exponential ones, the transformation of the three-body basis functions between the three rearrangement channels becomes very simple, and therefore six-dimensional integrations over the coordinates \mathbf{x} and \mathbf{y} for the matrix elements of Eq. (2.12) can be performed straightforwardly. The matrix elements of the norm overlap; the kinetic energy and the Coulomb potential are calculated fully analytically. As for the nuclear potential, the integration over five dimensions, $\hat{\mathbf{x}}$ and \mathbf{y} , are carried out analytically, and one-dimensional numerical integrations are left in the form of

$$\int_0^{\infty} x^{2m} e^{-a^2 x^2} v(x) x^2 dx, \quad (2.14)$$

where $v(x)$ denotes the radial dependence of the nuclear

potential, m being a non-negative integer. In this work, the numerical integration of (2.14) was performed with an accuracy of 10^{-7} MeV (here, we do not consider the error of the potential parameters). The whole numerical error in the binding energy generated up to the solution of Eq. (2.11) was examined and estimated to be less than 10^{-5} MeV. This accuracy is sufficiently high, and therefore a major source of error in this variational calculation (when greater than 10^{-5} MeV) is considered to be not from the numerical procedures but from the truncation of the wave-function space and degree of optimization of the nonlinear variational parameters.

The formulation of this method is rather general from the viewpoint of the variational approach. It is a kind of *ab initio* calculation; neither the two-nucleon correlation function nor the definite asymptotic form of the wave function is assumed *a priori*. A specific assumption is to take the radial basis functions to be of Gaussian shape [Eq. (2.13)] having geometrical-progression ranges. Numerical calculations required in this method are straightforward, as may be noticed from the expressions above.

III. INTERACTION AND MODEL SPACE

As an example of the realistic two-nucleon potential, we employ the AV14 potential⁶ for which precise results by the Faddeev calculations are available. In practical calculations, we have to truncate the space of trial functions by taking finite numbers of α in the expansion of Eq. (2.5). In this paper, we restrict the orbital angular momenta to $l_{\alpha} + L_{\alpha} \leq 6$, which results in 26 types of the configuration of Eq. (2.6). We refer to such configurations as channels, similar to the terminology of the Faddeev calculations. The 26 channels employed in our calculation are listed on the left-hand side (lhs) of Table I. In Secs. V and VI, we shall investigate convergence of the calculated results with respect to the increasing number of channels and compare it with the convergence of the Faddeev calculations. Hereafter, " N -channel" calculation of our method means a calculation with the use of the first N channels of Table I.

This calculation and the Faddeev one with the *same* number of channels cannot strictly be compared to each other, since the L - S coupling is taken in our calculation while the j - J coupling is adopted in the Faddeev cases. Nevertheless, such a comparison would be rather interesting. Then, arrangement of the channels in Table I is made as similarly as possible to that of the Faddeev channels, though the coupling schemes are different. Especially for the five-channel calculation, we take the same j - J coupling channels as in the Faddeev calculations; the five channels are composed of the first four ($\alpha=1-4$) of Table I and a specific combination of the

TABLE I. L - S coupling three-body channels, Eq. (2.6), and nonlinear variational parameters used in this work for ${}^3\text{H}$ and ${}^3\text{He}$.

Channel number	α	l_α	L_α	Λ_α	s_α	Σ_α	n_{\max}	x_{\min}	x_{\max}	N_{\max}	y_{\min}	y_{\max}
1	0	0	0	0	0	$\frac{1}{2}$	15	0.05	15.0	15	0.3	9.0
2	0	0	0	0	1	$\frac{1}{2}$	15	0.05	15.0	15	0.3	9.0
3	2	0	2	2	1	$\frac{3}{2}$	15	0.1	15.0	15	0.3	9.0
4	0	2	2	2	1	$\frac{3}{2}$	15	0.1	15.0	15	0.3	9.0
5	2	2	0	0	1	$\frac{1}{2}$	15	0.1	15.0	15	0.3	9.0
6	2	2	1	1	1	$\frac{1}{2}$	15	0.1	15.0	15	0.3	9.0
7	2	2	1	1	1	$\frac{3}{2}$	15	0.1	15.0	15	0.3	9.0
8	2	2	2	2	1	$\frac{3}{2}$	15	0.1	15.0	15	0.3	9.0
9	1	1	0	0	1	$\frac{1}{2}$	10	0.1	10.0	10	0.3	6.0
10	1	1	1	1	1	$\frac{1}{2}$	10	0.1	10.0	10	0.3	6.0
11	1	1	1	1	1	$\frac{3}{2}$	10	0.1	10.0	10	0.3	6.0
12	1	1	2	2	1	$\frac{3}{2}$	10	0.1	10.0	10	0.3	6.0
13	1	1	0	0	0	$\frac{1}{2}$	10	0.1	10.0	10	0.3	6.0
14	1	1	1	1	0	$\frac{1}{2}$	10	0.1	10.0	10	0.3	6.0
15	2	2	0	0	0	$\frac{1}{2}$	10	0.1	10.0	10	0.3	6.0
16	2	2	1	0	0	$\frac{1}{2}$	10	0.1	10.0	10	0.3	6.0
17	1	3	2	1	1	$\frac{3}{2}$	10	0.1	10.0	10	0.3	6.0
18	3	1	2	1	1	$\frac{3}{2}$	10	0.1	10.0	10	0.3	6.0
19	3	3	0	1	1	$\frac{1}{2}$	10	0.1	10.0	10	0.3	6.0
20	3	3	1	1	1	$\frac{1}{2}$	10	0.1	10.0	10	0.3	6.0
21	3	3	1	1	1	$\frac{3}{2}$	10	0.1	10.0	10	0.3	6.0
22	3	3	2	1	1	$\frac{3}{2}$	10	0.1	10.0	10	0.3	6.0
23	3	3	0	0	0	$\frac{1}{2}$	10	0.1	10.0	10	0.3	6.0
24	3	3	1	0	0	$\frac{1}{2}$	10	0.1	10.0	10	0.3	6.0
25	2	4	2	1	1	$\frac{3}{2}$	10	0.1	10.0	10	0.3	6.0
26	4	2	2	1	1	$\frac{3}{2}$	10	0.1	10.0	10	0.3	6.0

next four channels ($\alpha=5-8$).

It is to be emphasized here that, in the Faddeev calculations, partial-wave expansion of the interaction is performed and truncations of the partial waves are made; the partial waves with $j \leq 1^+$ (${}^1S_0, {}^3S_1, {}^3D_1$), $j \leq 2$, $j \leq 3$, and $j \leq 4$ are employed in the calculations with 5, 18, 26, and 34 channels, respectively. On the other hand, our method does *not* take such a partial-wave decomposition of the nuclear and Coulomb interactions, but incorporates the full interactions in the Hamiltonian (2.3).

In the case of the ${}^3\text{He}$ nucleus, we include the Coulomb potential in the Hamiltonian (2.3) and calculate the binding energy nonperturbatively; namely, the eigenvalue problem of Eqs. (2.11) is solved with the Coulomb matrix elements incorporated. Recently Wu, Ishikawa, and Sasakawa¹⁹ made a Faddeev calculation of ${}^3\text{He}$ in which the Coulomb potential is treated nonperturbatively. They took 6 (5), 28 (18), 38 (26), and 52 (34) channels, respectively, with the truncation of $j \leq 1^+$ (${}^1S_0, {}^3S_1, {}^3D_1$), $j \leq 2$, $j \leq 3$, and $j \leq 4$ for the partial waves of the two-nucleon and Coulomb potentials; both the $T=\frac{1}{2}$ and $\frac{3}{2}$ channels were employed, and the numbers in parentheses are those for the $T=\frac{1}{2}$ channels. According to their calculation, mixture of the $T=\frac{3}{2}$ states into the ${}^3\text{He}$ ground state is about 0.03% in probability. In this work, there-

fore, we ignore the $T=\frac{3}{2}$ states for simplicity of calculation.

IV. ASYMPTOTIC NORMALIZATION CONSTANTS

It has often been argued that asymptotic behavior of the variationally obtained trinucleon wave functions is rather poor even though the binding energy is satisfactorily good. It is then of particular interest to examine our calculated wave function in the asymptotic region.

In order to calculate the S - and D -wave asymptotic normalization constants of ${}^3\text{H}$ and ${}^3\text{He}$, we follow the definitions given by Friar *et al.*²⁰ The constants, C_S and C_D for ${}^3\text{H}$ and C_S^C and C_D^C for ${}^3\text{He}$, are defined by

$$\begin{aligned} \Psi({}^3\text{H}) \xrightarrow{y_1 \rightarrow \infty} & C_S N_{ZR} \frac{e^{-\beta y_1}}{y_1} \Phi_0^{(d)}(\mathbf{x}_1, \hat{y}_1) \\ & + C_D N_{ZR} \frac{e^{-\beta y_1}}{y_1} \left[1 + \frac{3}{\beta y_1} + \frac{3}{(\beta y_1)^2} \right] \\ & \times \Phi_2^{(d)}(\mathbf{x}_1, \hat{y}_1) \end{aligned} \quad (4.1)$$

and

$$\Psi({}^3\text{He}) \xrightarrow{y_1 \rightarrow \infty} C_S^C N_W \frac{W_{-\kappa, 1/2}(2\beta y_1)}{y_1} \Phi_0^{(d)}(\mathbf{x}_1, \hat{y}_1)$$

$$+ C_D^C N_W \frac{W_{-\kappa, 5/2}(2\beta y_1)}{y_1} \Phi_2^{(d)}(\mathbf{x}_1, \hat{y}_1). \quad (4.2)$$

Here, the function $\Phi_L^{(d)}(\mathbf{x}_1, \hat{y}_1)$ ($L=0,2$) is a product of the deuteron wave function, $\phi_1^{(d)}(\mathbf{x}_1)$, and the j - J coupling spin-orbit function of the deuteron and the remaining nucleon:²⁰

$$\Phi_L^{(d)}(\mathbf{x}_1, \hat{y}_1) = [[Y_L(\hat{y}_1) \otimes \chi_{1/2}(1)]_I \otimes \phi_1^{(d)}(\mathbf{x}_1)]_{1/2} \frac{\eta}{\sqrt{2}}, \quad (4.3)$$

where $I = \frac{1}{2}$ and $\frac{3}{2}$ for $L=0$ and 2 , respectively, and η is the isospin function of the three-nucleon system. In Eqs. (4.1) and (4.2), β and κ are determined by

$$\beta = \left[\frac{4M}{3\hbar^2} (B_3 - B_2) \right]^{1/2}, \quad \kappa = \frac{2M\alpha}{3\beta}, \quad (4.4)$$

where B_3 is the calculated binding energy of the trinucleon, B_2 is that of the deuteron, M is the nucleon mass ($\hbar^2/M + 41.47$ MeV fm²), and $\alpha = \frac{1}{137}$. In Eq. (4.2), $W_{-\kappa, j}(2\beta y_1)$ is the Whittaker function that behaves irregularly at the origin and decays exponentially for $y_1 \rightarrow \infty$, and N_{ZR} and N_W are normalization factors defined by²⁰

$$N_{ZR} = \sqrt{2\beta}, \quad (4.5)$$

$$N_W = N_{ZR} \left[\frac{\Gamma(3+\kappa)\Gamma(2+\kappa)}{2 {}_3F_2(\kappa, 2, 1+\kappa; 3+\kappa, 2+\kappa; 1)} \right]^{1/2},$$

where $\Gamma(z)$ is the gamma function and ${}_3F_2$ is a hypergeometric function. In the limit of $\kappa \rightarrow 0$, Eq. (4.2) becomes Eq. (4.1).

In order to investigate Eqs. (4.1) and (4.2) more tractably, the d -³H and d -³He overlap functions are introduced as

$$u_L(y_1) = (\Phi_L^{(d)}(\mathbf{x}_1, \hat{y}_1) | \Psi(^3\text{H}) \rangle, \quad (4.6)$$

$$u_L^C(y_1) = (\Phi_L^{(d)}(\mathbf{x}_1, \hat{y}_1) | \Psi(^3\text{He}) \rangle, \quad (4.7)$$

where $L=0$ and 2 . By comparing these two equations with Eqs. (4.1) and (4.2), we have²⁰

$$u_0(y_1) \xrightarrow{y_1 \rightarrow \infty} C_S N_{ZR} \frac{e^{-\beta y_1}}{y_1}, \quad (4.8a)$$

$$u_2(y_1) \xrightarrow{y_1 \rightarrow \infty} C_D N_{ZR} \frac{e^{-\beta y_1}}{y_1} \left[1 + \frac{3}{\beta y_1} + \frac{3}{(\beta y_1)^2} \right] \quad (4.8b)$$

for ³H and

$$u_0^C(y_1) \xrightarrow{y_1 \rightarrow \infty} C_S^C N_W \frac{W_{-\kappa, 1/2}(2\beta y_1)}{y_1}, \quad (4.9a)$$

$$u_2^C(y_1) \xrightarrow{y_1 \rightarrow \infty} C_D^C N_W \frac{W_{-\kappa, 5/2}(2\beta y_1)}{y_1} \quad (4.9b)$$

for ³He. We shall calculate $u_0(y_1)$ and $u_2(y_1)$ and compare them with the right-hand side (rhs) of Eq. (4.8) in a wide region of sufficiently large y_1 to determine C_S and

C_D ; the same is done for C_S^C and C_D^C with Eq. (4.9).

We shall estimate the distorted-wave parameter D_2 which is introduced^{20,21} as

$$D_2 = -\frac{1}{15} \int_0^\infty y_1^4 u_2(y_1) dy_1 / \int_0^\infty y_1^2 u_0(y_1) dy_1 \quad (4.10)$$

and similarly for D_2^C with the use of u_0^C and u_2^C . We shall also calculate the quantities \bar{D}_2 and \bar{D}_2^C which are defined by²⁰

$$\bar{D}_2 = C_D / \beta^2 C_S, \quad \bar{D}_2^C = C_D^C / \beta^2 C_S^C \cdot f(\kappa), \quad (4.11)$$

where

$$f(\kappa) = \frac{{}_6F_1(2, \kappa-2; 5+\kappa; -1)}{(4+\kappa)(3+\kappa){}_2F_1(2, \kappa; 3+\kappa; -1)} \xrightarrow{\kappa \rightarrow 0} 1. \quad (4.12)$$

V. NUMERICAL RESULTS FOR ³H

Computational time of our method is satisfactorily short, which enables us to make a careful and extensive optimization of the nonlinear variational parameters. The first eight channels of Table I are the most important both for binding energy and for asymptotic behavior of the wave function. A set of optimized nonlinear parameters are listed on the right-hand side of Table I. Around the values the calculated binding energy is not significantly sensitive; it becomes less sensitive as the number of channels increases. We therefore took the case of round numbers for the range parameters x_{\min} , x_{\max} , y_{\min} , and y_{\max} .

First of all, we made a calculation with the j - J coupling five channels that are the same as those in the Faddeev calculations (cf. Sec. III). The binding energy obtained by this method is 7.643 MeV, which is 0.19 MeV larger than that of the Faddeev calculation^{4,19,22} with the five channels. This energy difference comes from the fact that the partial waves of the interaction pair are restricted to $j \leq 1^+$ (¹S₀, ³S₁-³D₁) in the five-channel Faddeev calculation, but the full interaction is taken in this calculation.

Table II shows the calculated binding energy and probabilities of the S , S' , P , and D states in the cases of 5–26 channels. Results given by the Faddeev calculations^{4,19,22} are also shown; arrangement of the channels is different between our calculations and the Faddeev calculations, except for the five-channel case (cf. Sec. III). In Fig. 3 we plot the binding energy versus the number of channels to illustrate the degree of convergence of the energy. Also, Fig. 4 shows convergence of the probabilities of the S , S' , and D states versus the number of channels. It is seen that the binding energy given by our method converges at the case of 18 channels within 0.001 MeV; the converged energy (7.684 MeV) is consistent with the three values given by the 34-channel Faddeev calculations. All of the percentage probabilities of the S , S' , P , and D states given by our calculations exhibit a convergence at the 12-channel cases at the level of 0.01%; they are nearly the same as those by the Faddeev calculations with 26 and 34 channels.

In order to investigate the asymptotic behavior of the wave function, we compare, in Fig. 5, the lhs and rhs of

TABLE II. Calculated binding energy of ${}^3\text{H}$ and probabilities of the S , S' , P , and D states for different numbers of channels. The AV14 potential was used. The numbers in parentheses are not shown in the references but given here by subtracting the sum of the other percentages from 100%.

Number of channels	$B({}^3\text{H})$ (MeV)	P_S (%)	$P_{S'}$ (%)	P_P (%)	P_D (%)
Our calculation					
5	7.643	89.894	1.134	0.063	8.909
8	7.660	89.879	1.129	0.066	8.926
10	7.674	89.847	1.128	0.075	8.950
12	7.678	89.835	1.127	0.076	8.962
14	7.6818	89.833	1.127	0.076	8.965
16	7.6820	89.833	1.127	0.076	8.965
18	7.6836	89.831	1.126	0.076	8.966
20	7.6840	89.831	1.126	0.076	8.967
22	7.6843	89.830	1.126	0.076	8.968
24	7.6843	89.830	1.126	0.076	8.968
26	7.6844	89.830	1.126	0.076	8.968
Faddeev calculation (Ref. 22)					
5	7.441	(89.70)	1.36	0.08	8.86
9	7.569	(89.69)	1.32	0.08	8.91
18	7.573	(89.88)	1.14	0.08	8.90
26	7.667	(89.84)	1.12	0.08	8.96
34	7.670	(89.84)	1.12	0.08	8.96
Faddeev calculation (Ref. 4)					
5	7.45	89.70	1.35	(0.08)	8.87
18	7.58	89.88	1.14	(0.07)	8.91
26	7.67	89.84	1.12	(0.07)	8.97
34	7.68	89.85	1.12	(0.07)	8.96
Faddeev calculation (Ref. 19)					
5	7.440	89.66	1.41	0.07	8.86
18	7.576	89.83	1.19	0.07	8.90
26	7.658	89.80	1.17	0.08	8.95
34	7.673	89.79	1.17	0.08	8.96

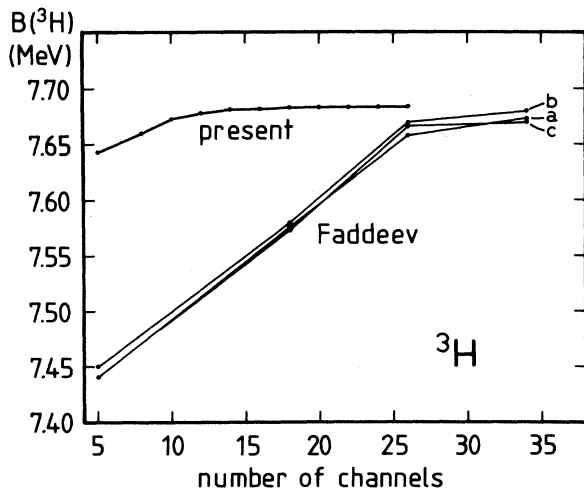


FIG. 3. Convergence of the calculated binding energy of ${}^3\text{H}$ with respect to the number of the three-body channels. The AV14 potential was used. Line a is taken from Ref. 19, b from Ref. 4, and c from Ref. 22.

Eq. (4.8) in the case of the 26-channel calculation [$B({}^3\text{H})=7.684$ MeV]; similar results were obtained in the other cases. The solid curves illustrate $u_0(y_1)$ and $u_2(y_1)$, and the dashed ones give the rhs functions of Eq. (4.8) with $C_S=1.827$ and $C_D=0.0740$. The values of C_S and C_D show good agreement with those by the Faddeev 34-channel calculation.^{4,23} We notice that $u_0(y_1)$ and $u_2(y_1)$ show accurate asymptotic behavior up to $y_1 \approx 17$ fm. Table III summarizes the values of the asymptotic normalization constants calculated by our wave functions with 5–26 channels, together with the results of the Faddeev calculations; our values of C_S and C_D are all estimated by normalizing the rhs function of Eq. (4.8) to the lhs one at $y_1=10$ fm; the relative error of C_S (C_D) due to the normalization at different positions ($y_1 \approx 8-17$ fm) is approximately 0.5% (0.7%). The asymptotic normalization constants obtained by our method depend very little on the number of channels, owing to the good convergence of binding energy.

In the last column of Table III, calculated distorted-wave parameters D_2 are listed. In the calculation of Eq.

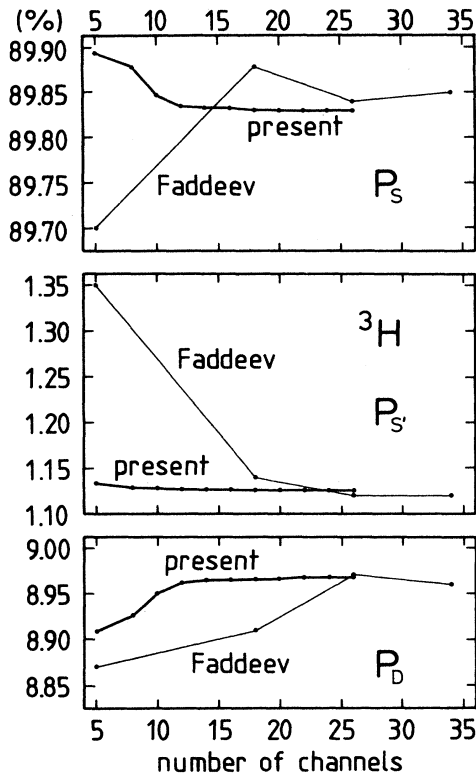


FIG. 4. Convergence of the probabilities of the S , S' , and D states of ${}^3\text{H}$ with respect to the number of three-body channels. The AV14 potential was used. The Faddeev results are taken from Ref. 4.

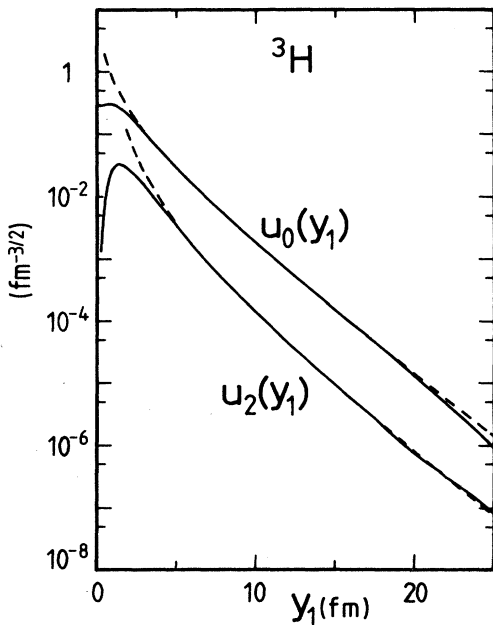


FIG. 5. Deuteron-triton overlap functions, $u_0(y_1)$ and $u_2(y_1)$, by the solid curves in the case of 26 channels. The dashed curves are rhs of Eq. (4.8) with C_S and C_D determined by the normalization at $y_1 = 10$ fm.

(4.10) we took the rhs of Eq. (4.8) for $y_1 \geq 17$ fm instead of the lhs (cf. Fig. 5); this affects the D_2 parameter by only $(2-3) \times 10^{-3} \text{ fm}^2$. Our calculation with five or more channels yields $D_2 = -0.226 \text{ fm}^2$, which agrees well with the result of the Faddeev calculation.⁴ In different types of variational calculations of the literature, the D_2 parameter has been estimated as -0.088 fm^2 by Jackson *et al.*,^{7,13} -0.088 fm^2 by Akaishi *et al.*,^{8,13} and -0.24 fm^2 by Schiavilla *et al.*¹² (C_S and C_D were not calculated there.) The last value of the D_2 parameter was estimated¹² with a Monte Carlo calculation of the momentum distribution of a variationally obtained three-body wave function, and is consistent with the results of our calculations and the Faddeev calculations. The first two values of the D_2 parameter cited above are critically small because of too rapid damping¹³ of $u_2(y_1)$ for $y_1 \gtrsim 6$ fm.

Finally, we make a speculation for the true value of the theoretical binding energy in the case of the AV14 potential used. From Tables I and II we see that contribution of the channels with $(l, L) = (1, 3)$ and $(3, 1)$ to the binding energy is 0.0016 MeV; the channels with $(l, L) = (3, 3)$ and those with $(l, L) = (2, 4)$ and $(4, 2)$ contribute by 0.0007 MeV and 0.0001 MeV, respectively, when they are successively added to the preceding channels in the order of Table I. The reason for this very minor role of the channels with $l+L=6$ is that all the partial waves of the two-body interaction are included in our Hamiltonian and that the *symmetrized* three-body basis functions in Eq. (2.8) with $l+L=6$ have a large overlap (nonorthogonality) with the set of basis functions with $l+L \leq 4$. We may therefore reasonably expect that the contribution of the channels with $l+L \geq 8$ which are not included in this work would be less than 10^{-4} MeV. We cannot neglect, however, the possibility that a much more extensive search of optimum nonlinear parameters of the channels with $l+L \leq 6$ would increase the binding energy by several 10^{-4} MeV. It is to be noted that since our method is based on the Rayleigh-Ritz variational principle, the calculated binding energy definitely increases as the number of channels increases (within numerical accuracy), and that the true value of the binding energy is predicted to be larger than the largest value by the variational calculation. Consequently, we speculate that the true value of the theoretical binding energy of ${}^3\text{H}$ with the use of the full AV14 potential may be 7.685 MeV.

From this viewpoint it is interesting to note that the values obtained by the recent 34-channel Faddeev calculation¹⁹ are close to our speculated true value. In the Faddeev method, the calculated binding energy does not necessarily increase with increasing number of channels, since the Hamiltonian itself changes as the number of channels increases; in fact, a sizable oscillation of the ${}^3\text{H}$ binding energy with respect to the number of channels is observed when a three-body force is incorporated.^{2,4} Therefore, it will be of particular interest to see convergence of the binding energy at the level of 0.001 MeV by increasing the number of the channels to more than 34, or to calculate the expectation value of the *full-interaction* Hamiltonian by the 34-channel Faddeev wave function.

TABLE III. Calculated normalization constants C_S and C_D of ${}^3\text{H}$ for different numbers of channels. The AV14 potential was used.

Number of channels	$B({}^3\text{H})$ (MeV)	C_S	C_D	C_D/C_S	\bar{D}_2 (fm ²)	D_2 (fm ²)
Our calculation						
5	7.643	1.825	0.0733	0.0402	-0.231	-0.226
8	7.660	1.825	0.0735	0.0403	-0.231	-0.226
10	7.674	1.826	0.0737	0.0403	-0.230	-0.226
12	7.678	1.827	0.0739	0.0404	-0.231	-0.226
14	7.682	1.828	0.0741	0.0405	-0.231	-0.226
16	7.682	1.827	0.0741	0.0405	-0.231	-0.226
18	7.684	1.827	0.0741	0.0405	-0.231	-0.226
20	7.684	1.827	0.0741	0.0405	-0.231	-0.226
22	7.684	1.827	0.0740	0.0405	-0.231	-0.226
24	7.684	1.827	0.0740	0.0405	-0.231	-0.226
26	7.684	1.827	0.0740	0.0405	-0.231	-0.226
Faddeev calculation (Ref. 23)						
5	7.44	1.813	0.0723	0.0399	-0.238	
9	7.57	1.825	0.0741	0.0406	-0.236	
18	7.57	1.815	0.0735	0.0405	-0.235	
34	7.67	1.821	0.0750	0.0412	-0.235	
Faddeev calculation (Ref. 4)						
5	7.45	1.81	0.0705	0.0390	-0.231	-0.221
18	7.58	1.82	0.0717	0.0395	-0.229	-0.219
26	7.67	1.82	0.0730	0.0401	-0.229	-0.223
34	7.68	1.82	0.0732	0.0402	-0.229	-0.221
Faddeev calculation (Ref. 19)						
5	7.440	1.81	0.0704	0.0390	-0.232	
18	7.576	1.81	0.0717	0.0396	-0.230	
26	7.658	1.81	0.0729	0.0402	-0.230	
34	7.673	1.82	0.0731	0.0403	-0.230	

VI. NUMERICAL RESULTS FOR ${}^3\text{He}$

The calculated ${}^3\text{He}$ binding energy is listed in Table IV together with the probability percentages of the S , S' , P , and D states. Results of the Faddeev calculations^{19,22} are also shown; in Ref. 22 the Coulomb force is treated perturbatively. The energy is illustrated in Fig. 6 with respect to the number of the $T=\frac{1}{2}$ channels. We see that $B({}^3\text{He})$ of our calculation converges at the 18-channel calculation within 0.001 MeV, which is the same as in the ${}^3\text{H}$ case. For ${}^3\text{He}$, we took the same parameters of the basis functions as in Table I; we examined other basis functions having longer ranges, but the value of $B({}^3\text{He})$ was not affected significantly. The basis functions of Table I are considered to be long enough in range to calculate all the quantities discussed in this paper; this will later be verified from the study of the asymptotic behavior of our ${}^3\text{He}$ wave function.

In Table IV and Fig. 6 we see that, at small numbers of the channels, the ${}^3\text{He}$ binding energy of our calculation is significantly larger than that of the Faddeev calculations.^{19,22} This is for the same reason as in the ${}^3\text{H}$ case that the partial waves of the nuclear and Coulomb in-

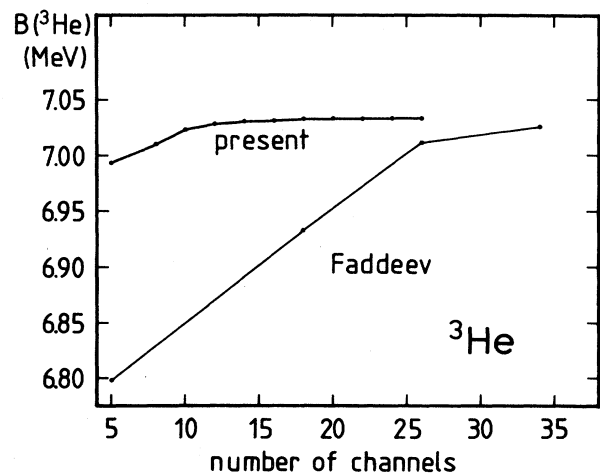


FIG. 6. Convergence of the calculated binding energy of ${}^3\text{He}$ with respect to the number of three-body channels with $T=\frac{1}{2}$. The AV14 potential was used. The result of the Faddeev calculation is taken from Ref. 19, which includes $T=\frac{3}{2}$ channels besides the $T=\frac{1}{2}$ ones.

TABLE IV. Calculated binding energy of ${}^3\text{He}$ and probabilities of the S , S' , P , and D states for different numbers of channels. The AV14 potential was used.

Number of channels	$B({}^3\text{He})$ (MeV)	ΔE_c (MeV)	P_S (%)	$P_{S'}$ (%)	P_P (%)	P_D (%)
Our calculation						
5	6.994	0.649	89.740	1.324	0.062	8.874
8	7.010	0.650	89.726	1.318	0.065	8.891
10	7.023	0.651	89.695	1.317	0.074	8.915
12	7.028	0.651	89.683	1.315	0.075	8.927
14	7.0309	0.651	89.681	1.315	0.075	8.929
16	7.0311	0.651	89.681	1.315	0.075	8.930
18	7.0326	0.651	89.680	1.315	0.075	8.931
20	7.0331	0.651	89.679	1.314	0.075	8.932
22	7.0333	0.651	89.679	1.314	0.075	8.932
24	7.0333	0.651	89.679	1.314	0.075	8.932
26	7.0334	0.651	89.679	1.314	0.075	8.932
Faddeev calculation ^a (Ref. 22)						
5	6.794	0.647				
9	6.918	0.651				
18	6.920	0.653				
26	7.011	0.656				
34	7.014	0.656				
Faddeev calculation ^b (Ref. 19)						
6(5)	6.799	0.641	89.54	1.58	0.07	8.80
28(18)	6.933	0.643	89.72	1.34	0.07	8.87
38(26)	6.012	0.647	89.69	1.32	0.07	8.92
52(34)	7.026	0.647	89.68	1.31	0.08	8.93

^a $B({}^3\text{He})$ is given by $B({}^3\text{H})$ plus ΔE_c calculated perturbatively.

^bThe numbers in parentheses are those of the channels with $T = \frac{1}{2}$.

teractions are truncated in the Faddeev calculation but not at all in this one. Particularly, the truncation for the Coulomb interaction might be an origin of slower convergence of the binding energy in ${}^3\text{He}$ than in ${}^3\text{H}$ seen in the Faddeev calculation of Ref. 19.

The calculated probabilities of the S , S' , P , and D states in ${}^3\text{He}$ converge at the case of 12 channels at the level of 0.01%, as seen in Table IV. Compared with the case of ${}^3\text{H}$, Coulomb effects slightly increase the probability of the mixed symmetric S' state and decrease that of the symmetric S state, with those of the P and D states unchanged.

In Fig. 7 we see that $u_0^C(y_1)$ and $u_2^C(y_1)$ show accurate asymptotic behavior up to $y_1 \approx 17$ fm. Table V lists the values of the asymptotic normalization constants calculated using our wave functions with 5–26 channels together with the results of the Faddeev calculations.^{19,23} The values of C_S^C and C_D^C are estimated by normalizing the rhs function of Eq. (4.9) to the lhs one at $y_1 = 10$ fm; there is some 0.5% (0.7%) error in the values of C_S^C (C_D^C) due to the normalization at different positions ($y_1 \approx 8$ –17 fm). \bar{D}_2^C and D_2^C do not depend on the number of channels, owing to the good convergence of $B({}^3\text{He})$. We recognize that the theoretical prediction²⁰ of $\bar{D}_2^C \approx D_2^C$, $\bar{D}_2 \approx D_2$, and $\bar{D}_2^C \approx \bar{D}_2$ holds well.

The Coulomb energy difference, $\Delta E_c = B({}^3\text{H}) - B({}^3\text{He})$, in our calculation with the AV14 potential is 0.651 MeV,

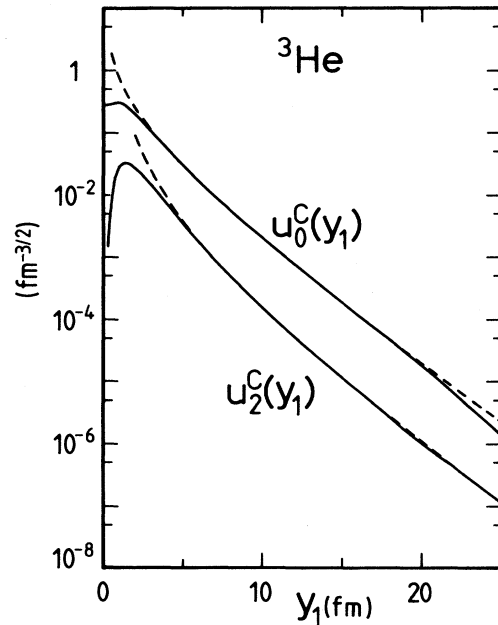


FIG. 7. Deuteron- ${}^3\text{He}$ overlap functions, $u_0^C(y_1)$ and $u_2^C(y_1)$, by the solid curves in the case of the 26 channels. The dashed curves are the rhs of Eq. (4.9) with C_S^C and C_D^C determined by the normalization at $y_1 = 10$ fm.

TABLE V. Calculated normalization constants C_S^C and C_D^C of ${}^3\text{He}$ for different numbers of channels. The AV14 potential was used.

Number of channels	$B({}^3\text{He})$ (MeV)	C_S^C	C_D^C	C_D^C/C_S^C	\bar{D}_2^C (fm ²)	D_2^C (fm ²)
Our calculation						
5	6.994	1.835	0.0698	0.0380	-0.240	-0.236
8	7.010	1.836	0.0700	0.0381	-0.240	-0.236
10	7.023	1.837	0.0701	0.0382	-0.239	-0.236
12	7.028	1.837	0.0703	0.0383	-0.240	-0.236
14	7.031	1.838	0.0705	0.0384	-0.240	-0.236
16	7.031	1.838	0.0705	0.0384	-0.240	-0.236
18	7.033	1.838	0.0705	0.0384	-0.240	-0.236
20	7.033	1.838	0.0705	0.0384	-0.240	-0.236
22	7.033	1.838	0.0704	0.0383	-0.240	-0.236
24	7.033	1.838	0.0704	0.0383	-0.240	-0.236
26	7.033	1.838	0.0704	0.0383	-0.240	-0.236
Faddeev calculation (Ref. 23)						
5	6.78	1.816	0.0681	0.0375	-0.248	
9	6.90	1.826	0.0692	0.0379	-0.244	
18	6.92	1.827	0.0698	0.0389	-0.245	
34	7.01	1.833	0.0715	0.0390	-0.245	
Faddeev calculation ^a (Ref. 19)						
6(5)	6.799	1.82	0.0658	0.0361	-0.238	
28(18)	6.933	1.82	0.0677	0.0371	-0.238	
38(26)	7.012	1.83	0.690	0.0377	-0.238	
52(34)	7.026	1.83	0.692	0.0378	-0.238	

^aThe numbers in parentheses are those of the channels with $T = \frac{1}{2}$.

which does not depend on the number of channels (when greater than ten as seen in Table IV) on account of good convergence of the binding energies. The Faddeev calculation of Ref. 19 yields $\Delta E_c = 0.669$ MeV in the case of truncation $j \leq 4$ for the partial waves of the nuclear and Coulomb potentials; convergence of the value is at the

level of 0.01 MeV compared with the case of truncation $j \leq 3$. It is to be noted that the $T = \frac{3}{2}$ channels are included in Ref. 19 but ignored in this paper, and that inclusion of the channels in our *variational* method is to make $B({}^3\text{He})$ definitely increase (even though possibly very little), resulting in the same amount of increase of ΔE_c .

TABLE VI. Contributions of the S , P , and D states to the kinetic, nuclear, and Coulomb energies. The AV14 potential was used. The numbers in parentheses are the first-order perturbation calculation of Coulomb energy of ${}^3\text{He}$ with the ${}^3\text{H}$ wave function.

Energy (MeV)	${}^3\text{H}$	${}^3\text{He}$
Kinetic	45.677	44.812
S		28.543
P		0.288
D		16.041
Nuclear	-53.360	-52.491
S		-16.496
P		0.056
D		2.598
$\langle S, P \rangle$		-0.007
$\langle S, D \rangle$		-38.071
$\langle P, D \rangle$		-0.568
Coulomb	(0.656)	0.646
S		0.592
P		0.001
D		0.053
Total	-7.684	-7.033

The effect of three-body potentials on the Coulomb energy difference will be of much interest.

Contributions of the S , P , and D states to the kinetic, nuclear, and Coulomb energies of ${}^3\text{He}$ are listed in Table VI, as are those for ${}^3\text{H}$. Here, the state S denotes the sum of the totally symmetric S state and the mixed symmetric S' state. Results of the 18-channel calculation are listed; but they are the same up to the 26-channel case except for small changes in the digit of 0.001 MeV. For the nuclear potential, nondiagonal contributions (the last three) are shown as well as the diagonal ones. Firstly, it is interesting to see that the dominant contribution (~ -38 MeV) of the nuclear interaction comes from the nondiagonal matrix elements between the S and D states, whereas the S -state contribution is much smaller (~ -16 MeV); the trinucleon systems are not bound with the part of the central potential alone. The slight difference in the spatial part of the wave functions between ${}^3\text{H}$ and ${}^3\text{He}$ due to the Coulomb interaction (cf. Tables II and IV) is found to give rise to approximately 1 MeV changes of both kinetic and nuclear-potential energies, but the changes almost cancel each other, resulting in the Coulomb energy difference, $\Delta E_c = 0.651$ MeV, being close to the estimation by the first-order perturbation, 0.656 MeV.

VII. SUMMARY AND CONCLUDING REMARKS

We have studied the ground state of ${}^3\text{H}$ and ${}^3\text{He}$ with the use of the coupled-rearrangement-channel Gaussian-basis variational method which was developed¹⁴ in the study of muonic molecular ions, Coulomb-interacting three-body systems. The method incorporates the full interaction with no partial-wave expansion, in contrast to the Faddeev equations method which restricts the partial waves of the nuclear and Coulomb interactions. In our method, the three-nucleon wave function is expressed as a symmetric sum of the three rearrangement-channel amplitudes which are expanded with basis functions of Jacobian coordinates of the individual channels. The expansion coefficients and the energy were determined by the Rayleigh-Ritz variational principle. The basis-function space was truncated, in a similar manner to the Faddeev method, with respect to the three-body angular-momentum channels. The radial parts of the basis functions were described with Gaussian-tail functions whose ranges are distributed in geometrical progressions from very short ranges through sufficiently long ones.

Calculations were made with the use of the AV14 potential; the Coulomb force is included nonperturbatively for ${}^3\text{He}$. It was found that our calculated results for the trinucleon binding energy and the probabilities of the S , S' , P , and D states show a fine convergence at 18 and 12 channels, respectively. The results agree with those of the Faddeev calculations with the truncation $j \leq 4$.^{4,19,22}

At a small number of channels, the binding energy obtained by our calculation is significantly larger than that obtained by the Faddeev calculation; for example, $B({}^3\text{H}) = 7.64$ MeV by the former and 7.45 MeV by the latter in the case of five channels. This difference comes from the fact that our method takes the full interaction, whereas the Faddeev method truncates the interactions in the angular momentum space. When three-body potentials are incorporated in the Faddeev calculation,^{2,4} convergence of the triton binding energy is rather slow and oscillatory. It is therefore particularly interesting to include such three-body potentials in the proposed full-interaction framework and examine the convergence; this calculation is in progress along with the study of Coulomb effects in this case.

It was a difficult problem in various variational methods to accurately describe both the short-range correlations and the asymptotic behavior of the trinucleon, even though the binding energy was obtained satisfactorily well. This problem has been solved by our method. The deuteron-trinucleon overlap functions were calculated and their asymptotic behaviors were explicitly examined; the functions are considered to be accurate up to a sufficiently large separation (~ 17 fm) of the deuteron and the remaining nucleon. Asymptotic normalization constants of ${}^3\text{H}$ and ${}^3\text{He}$ calculated by our method are consistent with the results of the Faddeev calculations.^{19,23} This success is owed to the use of the Gaussian basis functions having appropriate ranges given in the form of geometrical progressions.

One of the characteristics of our method is that the three-body wave function is described in terms of tractable functions which are extremely suitable for coordinate transformations and integrations. One can then easily utilize the wave function for some other purposes such as calculation of the form factors for electron scattering and nuclear reactions. [The coefficients $\{A_{\bar{\alpha}}\}$ in Eq. (2.8) are available on request.]

We have not discussed a comparison of the calculated asymptotic normalization constants with observed values. This is because of the following. It is known^{4,23} that there is a strong correlation between the asymptotic normalization constants and the binding energy. For a meaningful comparison it is then necessary to have a wave function which correctly reproduces the observed trinucleon binding energy; such a wave function may be obtained with the inclusion of an appropriate three-body force.

In order to confirm the usefulness of our three-body basis functions, we mention the following work under way.^{24,25} Using the same j - J coupling five-channel basis functions of this calculation for ${}^3\text{H}$, we solved the Faddeev equations by the following matrix eigenvalue problem for $\{A_{\bar{\alpha}}\}$ and E :

$$\sum_{\bar{\alpha}} \langle \Phi_{\bar{\alpha}}(\mathbf{x}_1, \mathbf{y}_1) | T + V(\mathbf{x}_1) - E | \Phi_{\bar{\alpha}}(\mathbf{x}_1, \mathbf{y}_1) \rangle A_{\bar{\alpha}} = - \sum_{\bar{\alpha}} \langle \Phi_{\bar{\alpha}}(\mathbf{x}_1, \mathbf{y}_1) | V(\mathbf{x}_1) | \Phi_{\bar{\alpha}}(\mathbf{x}_2, \mathbf{y}_2) + \Phi_{\bar{\alpha}}(\mathbf{x}_3, \mathbf{y}_3) \rangle A_{\bar{\alpha}},$$

where the notation is the same as in Sec. II except that $\sum_{\bar{\alpha}} A_{\bar{\alpha}} \Phi_{\bar{\alpha}}(\mathbf{x}_i, \mathbf{y}_i)$ ($i=1,2,3$) now stand for the Faddeev

amplitudes. We precisely reproduced^{24,25} the results of the five-channel Faddeev calculation of ${}^3\text{H}$ in binding en-

ergy, probabilities of the S , S' , P , and D states, and the S - and D -wave asymptotic normalization constants. Solution of the above equations for the 18, 26, and 34 channels is in progress along with calculation of the expectation value of the *full-interaction* Hamiltonian by the Faddeev wave function.

Application of the present variational method to the ${}^4\text{He}$ bound state is straightforward with both $3N+N$ and $2N+2N$ partitions taken into account. A preliminary calculation by us with the Malfliet-Tjon potential (MI-V) (Ref. 26) was reported in Refs. 24 and 27; the calculated binding energy (31.357 MeV) agrees with the results by the methods of Ref. 28 (31.36 MeV), Ref. 9 (31.36 MeV), and Ref. 29 (31.3 ± 0.2 MeV). The second 0^+ state, having a strongly dissociated $3N+N$ configuration, was obtained at $E_x = 22.86$ MeV, which may be compared with the resonant 0_2^+ state observed at $E_x = 20.1$ MeV.

Extension of this framework of coupled-rearrangement channels to scattering problems is of particular interest. An example is seen in the study³⁰ of the Coulomb-interacting muon transfer reaction,

$$(d\mu^-)_{1s} + t \rightarrow (t\mu^-)_{1s} + d + 48 \text{ eV} ,$$

at the incident energies of 0.001–10 eV where no inelastic-excitation channels are open. The Schrödinger equation of this problem was solved nonadiabatically with the use of a variational method of Kohn-Hulthén type which was developed in Ref. 31 for composite-particle scattering. This method is expected to be applic-

able to the N - d scattering below the deuteron breakup energy. For higher energies, proper treatment of three-body breakup continuum is necessary. For nuclear breakup reactions (not for the N - d case), one of the authors (M.K.) and the collaborators³² have developed a method of coupled discretized continuum channels (CDCC) and have successfully analyzed a variety of experimental data associated with breakup processes of deuterons and heavier projectiles. It will be interesting work to combine the CDCC method with our method of coupled-rearrangement channels and apply them to N - d scattering above the deuteron breakup energy.

ACKNOWLEDGMENTS

The authors wish to thank Professor M. Yahiro for helpful discussions on the asymptotic behavior of the three-nucleon wave functions. They also wish to thank Professor M. Kawai, Professor Y. Wakuta, and Professor T. Matsuse for their encouragement and discussions in the course of this study. The authors would like to acknowledge Professor T. Sasakawa, Dr. S. Ishikawa, and Mr. Y. Wu for valuable discussions from the viewpoint of the Faddeev equations method. This work was partially supported by the Institute of Plasma Physics, Nagoya University, and the Grant-in-Aid for Scientific Research. Numerical calculations were performed on FACOM VP-200 at the Computer Center of Kyushu University and on FACOM VP-200E at the Institute of Plasma Physics.

- ¹R. B. Wiringa, J. L. Friar, B. F. Gibson, G. L. Payne, and C. R. Chen, *Phys. Lett.* **143B**, 273 (1984).
²C. R. Chen, G. L. Payne, J. L. Friar, and B. F. Gibson, *Phys. Rev. C* **33**, 1740 (1986).
³S. Ishikawa, T. Sasakawa, T. Sawada, and T. Ueda, *Phys. Rev. Lett.* **53**, 1877 (1984); T. Sasakawa and S. Ishikawa, *Few-Body Syst.* **1**, 3 (1986).
⁴S. Ishikawa and T. Sasakawa, *Few-Body Syst.* **1**, 143 (1986).
⁵S. A. Coon, M. D. Scadron, P. C. McNamee, B. R. Barrett, D. W. E. Blatt, and B. H. J. McKellar, *Nucl. Phys.* **A317**, 242 (1979); S. A. Coon and W. Glöckle, *Phys. Rev. C* **23**, 1790 (1981).
⁶R. B. Wiringa, R. A. Smith, and T. A. Ainsworth, *Phys. Rev. C* **29**, 1207 (1984).
⁷A. D. Jackson, A. Lande, and P. U. Sauer, *Phys. Lett.* **35B**, 365 (1971); S. N. Yang and A. D. Jackson, *ibid.* **36B**, 1 (1971).
⁸Y. Akaishi, M. Sakai, J. Hiura, and H. Tanaka, *Prog. Theor. Phys. Suppl.* **56**, 6 (1974).
⁹Y. Akaishi, in *Models and Methods in Few-Body Physics*, Vol. 273 of *Lecture Notes in Physics*, edited by L. S. Ferreira, A. C. Fonseca, and L. Streit (Springer-Verlag, Berlin, 1987), p. 324.
¹⁰M. A. Hennel and L. M. Delves, *Nucl. Phys.* **A246**, 490 (1975).
¹¹P. Nunberg, D. Prosperi, and E. Pace, *Nucl. Phys.* **A285**, 58 (1977).
¹²J. Carlson, V. R. Pandharipande, and R. B. Wiringa, *Nucl. Phys.* **A401**, 59 (1983); R. Schiavilla, V. R. Pandharipande, and R. B. Wiringa, *ibid.* **A449**, 219 (1986).
¹³L. D. Knutson and S. N. Yang, *Phys. Rev. C* **20**, 1631 (1979).
¹⁴M. Kamimura, *Phys. Rev. A* **38**, 621 (1988).
¹⁵See, for example, L. I. Ponomarev, *At. Phys.* **10**, 197 (1987); L. I. Ponomarev, *Muon Catalyzed Fus.* **3**, 629 (1988).
¹⁶R. V. Reid, *Ann. Phys. (N.Y.)* **50**, 411 (1968).
¹⁷Y. Fukushima and M. Kamimura, *Proceedings of the International Conference on Nuclear Structure, Tokyo, 1977*, edited by T. Marumori [*J. Phys. Soc. Jpn. Suppl.* **44**, 225 (1978)]; M. Kamimura, *Nucl. Phys.* **A351**, 456 (1981).
¹⁸T. Matsuse and N. Hoshi, talk given at the Annual Meeting of Physical Society of Japan, Matsumoto, 1978; and private communication.
¹⁹T. Sasakawa, in *Proceedings of the Workshop on Electron-Nucleus Scattering, Elba International Physics Center, Italy, 1988*; Y. Wu, S. Ishikawa, and T. Sasakawa (private communication).
²⁰J. L. Friar, B. F. Gibson, D. R. Lehman, and G. L. Payne, *Phys. Rev. C* **25**, 1616 (1982).
²¹L. D. Knutson, B. P. Hichwa, A. Barroso, A. M. Eiro, F. D. Santos, and R. C. Johnson, *Phys. Rev. Lett.* **35**, 1570 (1975).
²²C. R. Chen, G. L. Payne, J. L. Friar, and B. F. Gibson, *Phys. Rev. C* **31**, 2266 (1985).
²³J. L. Friar, B. F. Gibson, L. R. Lehman, and G. L. Payne,

- Phys. Rev. C **37**, 2859 (1988).
- ²⁴H. Kameyama, Ph.D. thesis, Kyushu University, 1989.
- ²⁵M. Yahiro, H. Kameyama, and M. Kamimura, in Abstracts of the Annual Meeting of Physical Society of Japan, Hiratsuka, 1989.
- ²⁶R. A. Malfliet and J. A. Tjon, Nucl. Phys. A**127**, 161 (1969).
- ²⁷H. Kameyama, Y. Fukushima, M. Kamimura, in Contributions of the Fifth International Conference on Clustering Aspects in Nuclear and Subnuclear Systems, Kyoto, July, 1988, pp. 338 and 436.
- ²⁸J. G. Zabolitzky, Phys. Lett. **100B**, 5 (1981).
- ²⁹J. Carlson, Phys. Rev. C **36**, 2026 (1987).
- ³⁰M. Kamimura, Muon Catalyzed Fus. **3**, 822 (1988).
- ³¹M. Kamimura, Prog. Theor. Phys. Suppl. **62**, 236 (1977).
- ³²M. Kamimura, M. Yahiro, Y. Iseri, Y. Sakuragi, H. Kameyama, and M. Kawai, Prog. Theor. Phys. Suppl. **89**, 1 (1986); M. Kamimura, M. Yahiro, Y. Iseri, Y. Sakuragi, H. Kameyama, M. Kawai, and M. Tanifuji, in Proceedings of the International Nuclear Physics Conference, Harrogate, 1986, edited by J. L. Durell, J. M. Irvine, and G. C. Morrison, 1987, p. 483; N. Austern, Y. Iseri, M. Kamimura, M. Kawai, G. Rawitscher, and M. Yahiro, Phys. Rep. **154**, 125 (1987).